

Mimicked scaffolds based on coated silk woven fabric with gelatin and chitosan for soft tissue defect in oral maxillofacial area

Supaporn Sangkert¹, Suttatip Kamolmatyakul²
and Jirut Meesane¹ 

The International Journal of Artificial
Organs
2020, Vol. 43(3) 189–202
© The Author(s) 2019
Article reuse guidelines:
sagepub.com/journals-permissions
DOI: 10.1177/0391398819877191
journals.sagepub.com/home/jao


Abstract

Soft tissue defects in the oral maxillofacial area are critical problems for many patients and, in some cases, patients require an operation coupled with a performance scaffold substitution. In this research, mimicked anatomical scaffolds were constructed using gelatin- and chitosan-coated woven silk fibroin fabric. The morphologies, crystals, and structures were observed and then characterized using scanning electron microscopy, X-ray diffraction, and differential scanning calorimetry, respectively. Physical performance was evaluated from the swelling behavior, mechanical properties, and biodegradation, while the biological performance was tested with fibroblasts and keratinocytes, after which cell proliferation, viability, and histology were evaluated. The results revealed that a coated woven silk fibroin fabric displayed a crystal structure of silk fibroin with amorphous gelatin and chitosan layers. Also, the coated fabrics contained residual water within their structure. The physical performance of the coated woven silk fibroin fabric with gelatin showed suitable swelling behavior and mechanical properties along with acceptable biodegradation for insertion at a defect site. The biological performances including cell proliferation, viability, and histology were suitable for soft tissue reconstruction at the defect sites. Finally, the results demonstrated that mimicked anatomical scaffolds based on a gelatin layer on woven silk fibroin fabric had the functionality that was promising for soft tissue construction in oral maxillofacial defect.

Keywords

Biomaterials, oral and maxillofacial silk fibroin, gelatin, chitosan, soft tissue engineering, mimicking

Date received: 15 May 2019; accepted: 27 August 2019

Introduction

Currently, many patients suffer from tissue defects at the mucosa from either trauma or disease in maxillofacial tissue.^{1–3} In severe cases, patients require surgery using a bio-material substitution to fit the defect area.⁴ Tissue engineering scaffolds are attractive biomaterials for the promotion of new tissue regeneration.⁵ Therefore, the creation of surgically functional scaffolds for tissue engineering in mucosa reconstruction becomes a challenge for surgeons as well as material scientists.

Tissue engineering scaffolds, for mucosa reconstruction, have often been constructed into two-dimensional (2D) layers.⁶ These sheet structures need to allow for regeneration of new tissue. Furthermore, 2D scaffolds need the geometry to

fit the anatomical structure of soft tissue.⁷ The anatomical structure of the mucosa has two main phases of keratinocytes and fibroblasts; however, scaffolds as an anatomical structure for soft tissue have been rarely reported.⁸ Hence, the construction of these scaffolds for soft tissue regeneration in maxillofacial surgery is presented in this research.

¹Faculty of Medicine, Institute of Biomedical Engineering, Prince of Songkla University, Hat Yai, Songkhla, Thailand

²Faculty of Dentistry, Department of Preventive Dentistry, Prince of Songkla University, Hat Yai, Songkhla, Thailand

Corresponding author:

Jirut Meesane, Faculty of Medicine, Institute of Biomedical Engineering, Prince of Songkla University, Hat Yai, Songkhla 90110, Thailand.
Email: jirutmeesane999@yahoo.co.uk

Mimicking is an attractive approach, which has been used to create performance scaffolds since mimicked scaffolds have the unique ability to enhance tissue formation.⁹ Some research has demonstrated that mimicked scaffolds could induce tissue formation in soft tissue.¹⁰ Therefore, due to its potential, mimicking was used to create 2D scaffolds in this research. Especially, our created 2D scaffolds mimicked the anatomy of native soft tissue, which has a bilayer of keratinocytes and fibroblasts.¹¹

Silk fabric has unique physical, mechanical, and biological performance capabilities that are suitable for biomaterial applications.¹² Silk fabrics also show suitable performance for construction into tissue engineering scaffolds.¹³ Since very few reports exist on the application of silk fabric for soft tissue engineering,¹⁴ we present silk fabric as a 2D scaffold for tissue engineering in mucosa surgery.

Gelatin is a natural protein that is often used in biomaterial applications¹⁵ because of the unique biofunctionality to induce cell adhesion and proliferation and as such gelatin has been fabricated into scaffolds for various types of tissue engineering, particularly in mucosa reconstruction.^{16,17} For soft tissue engineering, gelatin is often prepared into sheet scaffolds⁷ and so, based on those unique functionalities, gelatin was selected as the material to be combined with silk fabric for the construction of 2D scaffolds in this research.

Chitosan is a natural polymer that is functional, biocompatible, biodegradable, and nontoxic. These characteristics make it suitable for biomaterial applications,¹⁸ and for this reason chitosan is often fabricated into scaffolds for tissue engineering.¹⁹ For soft tissue, chitosan is prepared into sheet scaffolds to induce new tissue regeneration.²⁰ Furthermore, chitosan is chosen in combination with silk fabric for 2D scaffolds in the use of tissue engineering for mucosa surgery.

In this research, mimicked anatomical scaffolds of coated silk fibroin fabric (SF) in combination with gelatin and chitosan were evaluated for their morphological and structural organization as well as physical and biological performance.

Methods

Coating the SF

The SF was cut into $1.0 \times 1.0 \text{ cm}^2$ pieces. These pieces were then coated with 3% (w/v) of gelatin and chitosan solutions. The gelatin solution was prepared by dissolving gelatin powder (gelatin from porcine skin; Sigma-Aldrich) in distilled water at 50°C for 15 min.²¹ For preparation of the chitosan solution, acetic acid (0.1 M) was used to dissolve the chitosan (%DD $\geq 90\%$; Marine Bio Resources Co., Ltd. Thailand).²² Afterwards, the chitosan solution was filtered with cheesecloth. For the coating of SF, there were two steps. First, each SF was immersed in each solution for 30 min at 37°C . Second, the immersed SF was put in hydrophobic plastic molds before 1 mL of each solution was dropped onto the top of the pieces of fabric. Then,

Table 1. The experimental groups.

Groups	Detail
SF	Silk fabric
SF-GT	Gelatin-coated silk fabric
SF-CS	Chitosan-coated silk fabric

they were allowed to dry at room temperature for 24 h. The experiment groups are as shown in Table 1.

Scanning electron microscope

In all the groups, the surface and morphological structures of the fabrics were observed with a scanning electron microscope (SEM; Quanta400; FEI, Czech Republic). The samples were coated with gold using a gold sputter coater machine (SPI Supplies, Division of Structure Probe Inc., USA).

Swelling property

All groups of fabrics were soaked in a phosphate-buffered saline (PBS) solution at different time points: 0.5, 1, 2, 4, 8, 12, and 24 h. The weights of the fabrics were collected at before and after soaking in the PBS. The swollen samples were weighed immediately and the swelling ratios were calculated using the following equation²³

$$\text{Swelling ratio} = \frac{W_s - W_d}{W_d}$$

where W_s and W_d are the weights of the swollen scaffold and the dry scaffold, respectively.²⁴

Degradation properties

Lysozyme powder was dissolved at a concentration of 4 mg/mL (pH 7.4) with distilled water at room temperature. Then, the $1 \times 1 \text{ cm}^2$ pieces of scaffolds were immersed in the lysozyme solution and incubated at 37°C for 7, 14, 21, and 28 days. Afterwards, the scaffolds were washed in distilled water 2–3 times and frozen at -20°C prior to freeze-drying. The weight loss was calculated using the following equation

$$\text{Percentage of weight loss} = \frac{(\text{Initial weight} - \text{Weight after degradation}) \times 100}{\text{Initial weight}}$$

Tensile property testing

The silk fabric was cut into $1 \times 5 \text{ cm}^2$ pieces and fixed with glue onto a plastic plate. The tensile property of the sample was evaluated by a Lloyd Instrument under the condition of 10 N/min.

Fourier transform infrared characterization

Molecular organization of the woven SF, woven SF coated with gelatin (SF-GT), and woven SF coated with chitosan (SF-CS) were analyzed by Fourier transform infrared (FTIR) spectrophotometer using the EQUINOX 55 (Bruker Optics, Germany). The samples were prepared into a KBr pellet before being analyzed with an FTIR spectrophotometer in the range of 4000–400 cm^{-1} .

Differential scanning calorimetry characterization

The membranes were kept in a desiccator for 24 h. The membranes were then cut into small pieces and the samples were weighed and put into an aluminum pan. Differential scanning calorimetry (DSC; DSC7; PerkinElmer, USA) was used for sample characterization. The heat scanning was done from 20°C to 350°C.

X-ray diffraction characterization

The structures of the SF, SF-GT, and SF-CS were analyzed by X-ray diffraction (XRD; X'Pert MPD; Philips, The Netherlands). Samples were placed in the XRD instrument, whereas diffraction patterns were measured over a 2θ range of 5 θ –90 θ with a step size of 0.05 θ coupled with time per step of 1 s.

Cell culture experiments

In this study, the murine fibroblast L929 cell line was used for the biological function of the fabrics. The murine fibroblast L929 cell line was cultured in alpha-minimum essential medium (α -MEM; Gibco Ltd and Invitrogen, USA) with the addition of 1% penicillin/streptomycin, 0.1% amphotericin B, and 10% fetal bovine serum at 37°C in a humidified 5% of CO_2 and 95% air incubator. The murine fibroblast L929 cell line was seeded with a 2×10^4 /silk fabric and the medium was changed every 3–4 days.²⁵

The H357 keratinocyte cell line was cultured in Dulbecco's modified Eagle's medium (DMEM) combined with Ham's F-12 nutrient mixture, which was supplemented with 10% fetal calf serum, epidermal growth factor (10 ng/mL), hydrocortisone (0.5 g/mL), penicillin (100 U/mL), streptomycin (100 g/mL), and amphotericin B (2.5 g/mL).²⁶

Cell proliferation assay (PrestoBlue®; days 1, 3, 5, and 7)

The cell proliferations of the L929 and H357 cell lines in each SF were observed by PrestoBlue assay²⁷ (PrestoBlue Cell Viability Reagent; Invitrogen) according to the manufacturer's instructions.

After cell seeding at days 1, 3, 5, and 7 the media was removed and washed twice with 1X PBS upon which

1/10th volume of PrestoBlue reagent was added directly into the complete media and incubated for 1 h at 37°C. The proliferation rates of the cells were measured by monitoring the wavelength absorbance at a 600 nm emission.

Cell viability (fluorescence microscope on days 3, 5, and 7)

Since fluorescein diacetate (FDA) stains the extracellular matrix, FDA was used to observe the cell migration as well as the viability of the L929 fibroblasts and H357 keratinocytes in the silk fabrics. FDA powder was dissolved in acetone at 5 mg/mL. A quantity of 5 μL of FDA solution was added to the silk fabric in 1 mL of fresh media. After that, the excess FDA was removed by washing with 1X PBS. Following this, the fabrics were put on glass slides and observed under a fluorescence microscope.²⁸

Histology

In all groups of silk fabric, the L929 fibroblast cells and H357 keratinocytes were stained with haematoxylin and eosin (H&E) at days 3 and 5 for observation of the morphologies. Moreover, the collagen deposition of L929 fibroblasts was detected with Masson's trichrome staining on days 14 and 28. All groups of fabrics were immersed in paraffin after fixing with 4% formaldehyde at 4°C for 24 h. The paraffin blocks were then cut into 5- μm sections and positioned on glass slides. The slides were deparaffinized and hydrated for H&E and Masson's trichrome staining.²⁹

Statistical analysis

Statistical methods were used to analyze the mechanical properties, swelling, degradation, and cell proliferation. Five samples were used for each test. The samples were measured and statistically compared by one-way analysis of variance (ANOVA) and Tukey's honestly significant difference (HSD) test (SPSS 16.0 software package). A p -value less than 0.05 was accepted as statistically significant.

Results

Morphology of the scaffolds

After construction of the silk fabrics into mimicked anatomical biphasic scaffolds (Figure 1), their morphological structures were observed by SEM. The results revealed that the SF had the geometry of a woven structure (Figure 2(a)–(d)). The morphological structures of the SF-GT and SF-CS showed coated fiber bundles of woven SF (Figure 2(e)–(j)). Some free spaces between the bundles of fiber were filled by gelatin and chitosan. The coatings of gelatin and chitosan covered the entire woven SF (Figure 2(g)–(l)). Some areas of the covered surface had a twisted pattern of fiber bundles (Figure 2(h) and (l)).

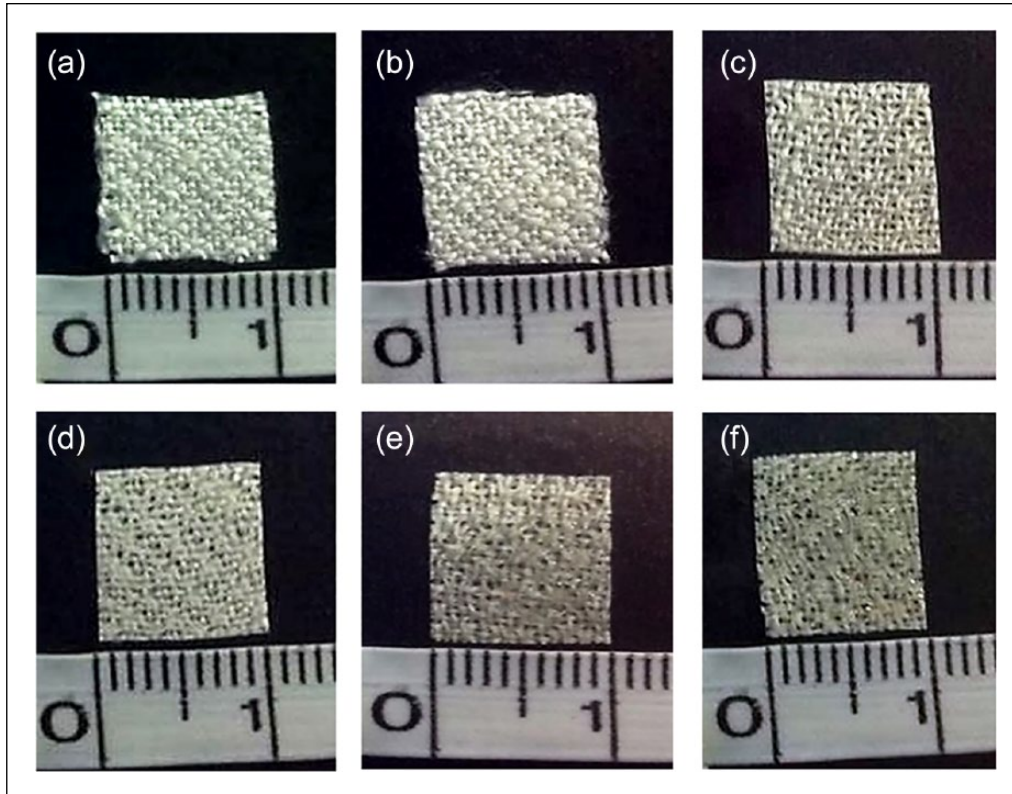


Figure 1. (a, d) Non-coated side of silk fabric. (b) Non-coated side of silk fabric with gelatin. (c) Non-coated side of silk fabric with chitosan. (e) Coated side of silk fabric with gelatin. (f) Coated side of silk fabric with chitosan.

Crystal structure characterization with XRD

The crystal structures of the mimicked, anatomical, biphasic scaffolds were characterized by XRD (Figure 3). The crystal analysis showed a peak at around 20° . Furthermore, this peak indicated that the beta-sheet conformation of silk fibroin was to be found in all groups.³⁰ The SF-GT and SF-CS had shoulders at around 20° – 40° .

Molecular structural characterization with DSC

The structural formations on mimicked, anatomical, biphasic scaffolds were characterized by DSC (Figure 4). Scanning was done in the temperature range of 27°C – 300°C , which covered the thermal behaviors of gelatin and chitosan.³¹ The DSC thermograms showed that all samples had peaks at around 50°C – 60°C . The peaks at 65.4° , 63.6°C , and 59.4°C represented the hydration of the SF, SF-GT, and SF-CS, respectively.^{32–34}

Swelling behavior of the scaffolds

The swelling behavior was chosen to evaluate the physical performance of the mimicked, anatomical, biphasic scaffolds (Figure 5). In the first 30 min, the SF revealed higher water absorption than either the SF-GT or SF-CS. This occurred because of the free spaces between the bundles of

the woven SF. Furthermore, the loose structure in those bundles also supported water absorption. The coated SF-GT fabric showed greater swelling than the SF-CS, which indicated that the gelatin coating had more water absorption than the chitosan coating. The SF-GT showed rapid swelling at around 30–60 min.

Biodegradation of the scaffolds

Lysozyme was used to evaluate the degradation in the biphasic sheets. After degradation with lysozyme, the SF did not degrade as much as the others (Figure 6), whereas high degradation was found in the groups of SF-GT and SF-CS. On day 7, degradation of the SF-GT was significantly higher than the SF-CS because the gelatin was actively degraded by the lysozyme at an early stage. However, degradation of the gelatin showed a similar rate as the chitosan after a prolonged time.

Mechanical behavior of the scaffolds

In this research, tensile testing was selected to evaluate the mechanical properties of the mimicked scaffolds. The initial results showed that the SF had greater extension at an earlier stage than the others as according to the stress–strain curve (Figure 7). This might have arisen from the loose

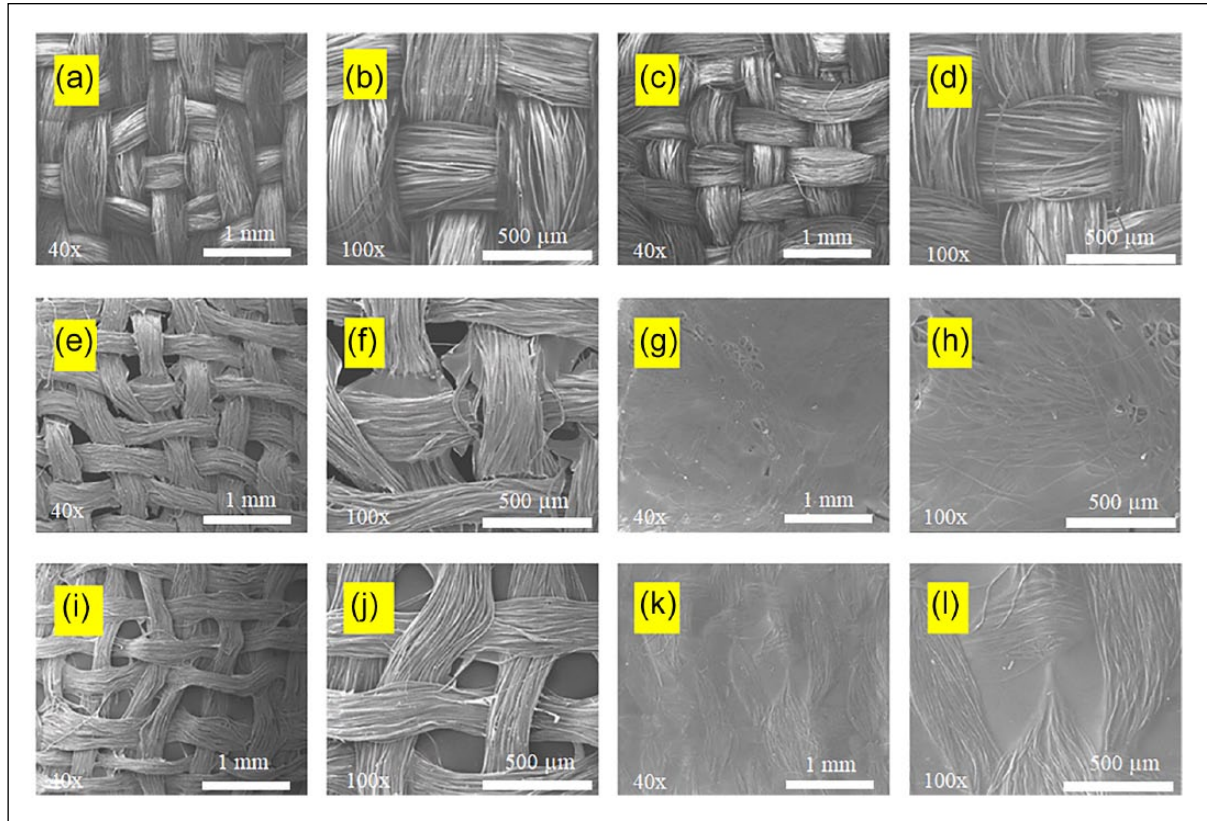


Figure 2. Surface morphology of coated silk fabric. (a–d) Non-coated side of silk fabric. (e, f) Non-coated side of silk fabric with gelatin. (g, h) Coated side of silk fabric with gelatin. (i, j) Non-coated side of silk fabric with chitosan. (k, l) Coated side of silk fabric with chitosan.

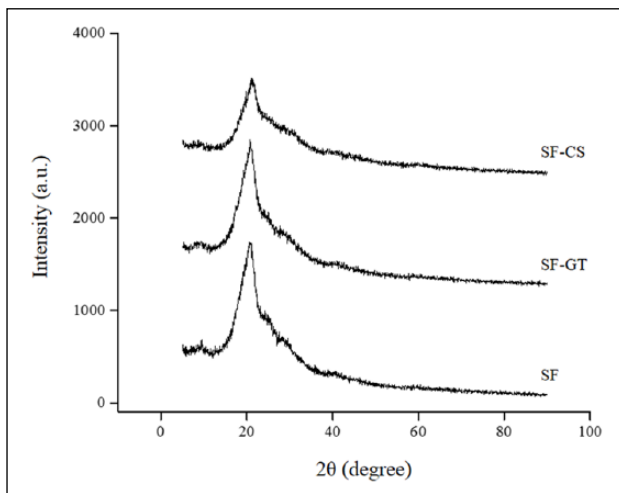


Figure 3. XRD spectra of silk fabric: SF, SF-GT, and SF-CS.

structure between the bundles of fibers leading to the greater extension of the SF at the early stage. Also, the SF had more difficult extension than the others, since the extension started after around 3% of strain. This possibly came from the loose structure of the SF, which showed more alignment of the fibers than the others. Therefore, that

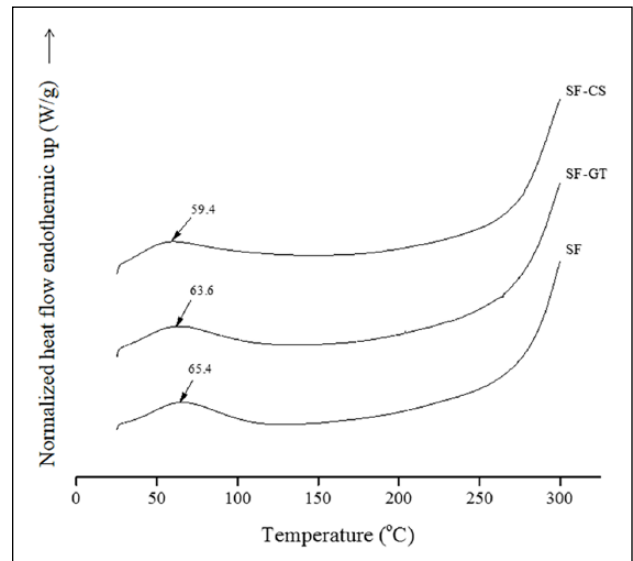


Figure 4. DSC thermograms of silk fabric: SF, SF-GT, and SF-CS.

alignment could induce rapid stress increase, which in turn led to the difficult extension. Afterwards, the SF started to break at a lower extension than the others. Again, this could

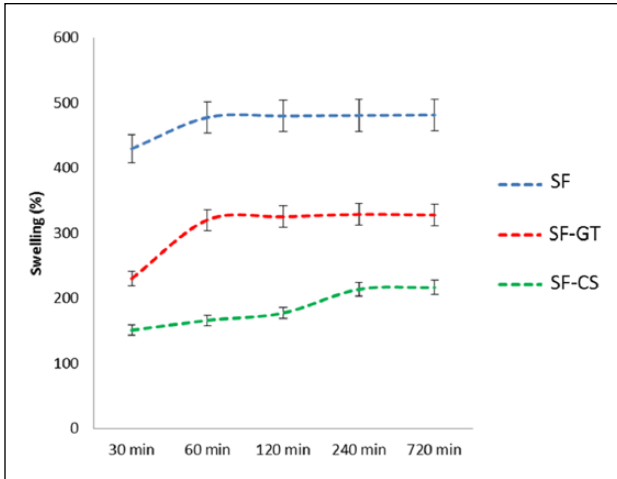


Figure 5. Swelling properties of silk fabric in all groups from 30 to 720 min in a PBS solution.

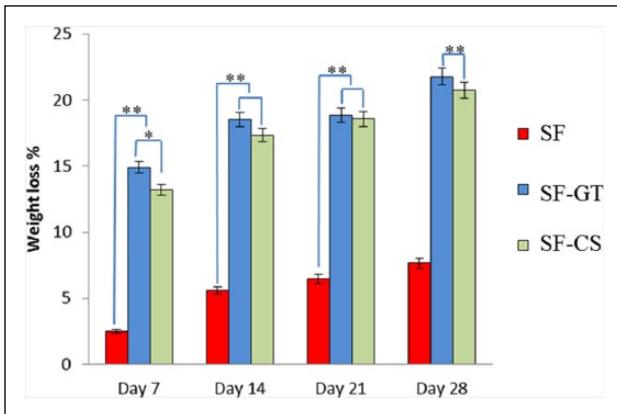


Figure 6. Degradation of silk fabric by lysozyme at different time points on days 7, 14, 21, and 28.

have occurred because of the uncoated SF fiber which was not shielded by the coatings. This was possibly the cause for the SF breaking at the lower extension. However, the SF-CS and SF-GT had hard extensions at the early stage but the SF-GT had a more difficult extension than the SF-CS at the early stage. Next, the mechanical properties were presented as a histogram (Figure 7(b)–(d)). The results showed that SF had the highest Young's modulus. However, SF-GT showed the lowest Young's modulus. Stress at the maximum load of SF-CS showed the highest value. There was no significant difference in stress at the maximum load between the SF and SF-GT. Finally, the results demonstrated that the SF-GT and SF-CS had more strain at the maximum load than the SF.

Fibroblast cell proliferation of the woven SF layer

Fibroblast proliferation on the woven silk layers of the SF-GT and SF-CS groups continuously increased from days 1 to 5 and then decreased on day 7. On day 1,

proliferation on the SF-GT was significantly higher than the SF and SF-CS (Figure 8). This was possibly derived from the bioactive functionality of gelatin and silk fibroin which can induce cell proliferation.^{35,36} On day 3, all groups revealed a similar action of cell proliferation with the exception of the SF-CS. Proliferation on the SF-GT was significantly higher than in the other groups and was representative of the cell behavior on day 5. Cell proliferation on day 7 of the SF was significantly different than in the other groups with a slight increase in the SF-GT. However, the SF-CS showed a decrease in cell proliferation.

Fibroblast cell viability of the woven silk fabric layer

Cell viability was selected to evaluate the biological performance of the mimicked, anatomical, biphasic scaffolds. The results showed fibroblast adhesion on the surface of the uncoated SF as well as the coated silk woven fabrics (Figure 9). The SF and SF-GT showed more unique fibroblast adhesion on the surface than the SF-CS from days 1 up to 7. The SF-GT had more fibroblast adhesion than the SF in the early stage at day 1.

Histological organization on the woven silk fabric layer

The morphology of the fibroblast was observed on the uncoated side at days 3 and 5 (Figure 10). On day 3, the results showed that the SF and SF-GT groups clearly had cell adhesion coupled with elongation on the surface. The SF-CS had clusters of cell aggregation; however, these were not elongated on the surface. This indicated that the surfaces of the SF and SF-GT showed suitable structures plus characteristics to promote both adhesion and elongation of the fibroblasts. On day 5, the dense cell adhesion and elongation was found on the surfaces of the SF and SF-GT. The fibroblasts showed a deeper migration into the bundles of the silk fibers of the SF-GT compared with that of the SF and SF-CS.

Masson's trichrome staining was used to evaluate the deposited collagen³⁷, which was synthesized by the fibroblasts on the silk fabrics in all groups (Figure 11). On day 14, it was clear that the SF-GT revealed more collagen deposition than the others. However, no collagen deposition was evident on the surface of the SF-CS. The cells expressed distribution over the entire surface of the SF and SF-GT, whereas the SF-CS had clusters of cell aggregation on the surface. On day 28, the SF-GT clearly showed collagen deposition that adhered to the fibrous bundles on the surface of the woven silk fabric. Furthermore, the collagen was diffused and deposited into the free spaces of the fibrous bundles. The SF demonstrated collagen and matrix nodules which adhered and spread on the fibrous bundles. Little collagen deposition was found in the SF-CS.

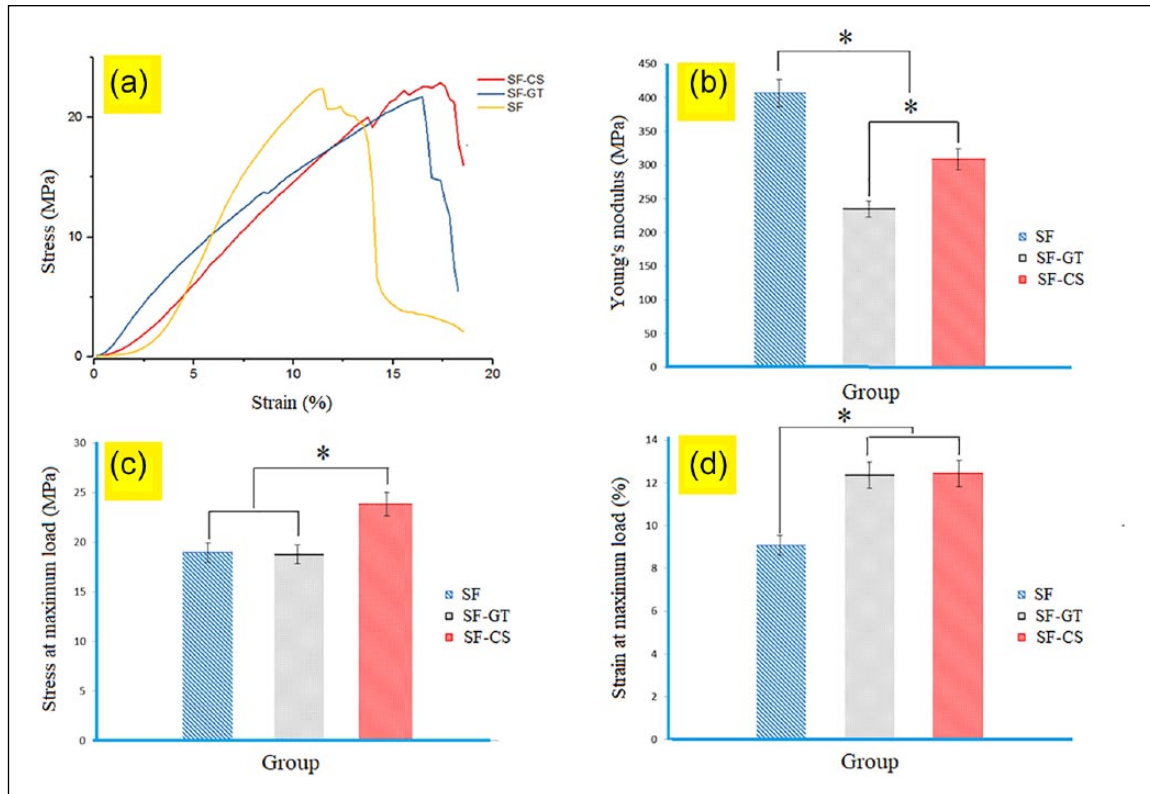


Figure 7. (a) Stress–strain curve. (b) Young's modulus. (c) Stress at maximum load. (d) Strain at maximum load of silk fabric in each group.

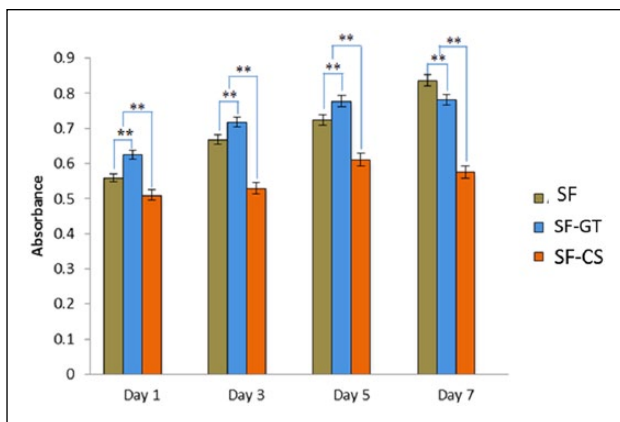


Figure 8. Fibroblast cell proliferation in the silk fabric on days 1, 3, 5, and 7.

Keratinocyte cell proliferation on the coated layers

The cell proliferation of the keratinocytes on the coating layer was performed on days 1, 3, 5, and 7 (Figure 12). On day 1, the SF-GT showed more cell proliferation than the other groups. Contrary to this, the SF-CS showed the least amount of cell proliferation. The highest cell proliferation was clearly found on day 5, and the SF-GT had the highest amount of cell proliferation.

Keratinocyte cell viability of the coating layer

Keratinocyte staining with FDA was used to observe the cell viability on the silk fabrics for all groups on days 1, 3, and 5 (Figure 13). The SF and SF-GT clearly showed more cell attachment on the surface than the SF-CS at all time points. The SF and SF-GT showed cell migration which covered the entire surfaces on days 3 and 5.

Histological organization on the coating layer

The morphologies of the keratinocytes on the coated layers were observed at days 3 and 7. The results showed that the SF, SF-GT, and SF-CS supported cell adhesion as well as migration. On day 7, the SF-GT had more cell attachment than the SF and SF-CS. The morphology of the keratinocytes showed a spherical pattern compared with the fibroblast cells; in addition, the SF-GT also showed the greatest cell aggregation compared to the others (Figure 14).

Discussion

Morphological and structural formation of the mimicked scaffolds

The mimicked anatomical scaffolds for soft tissue defect surgery were constructed in two parts. The first part was

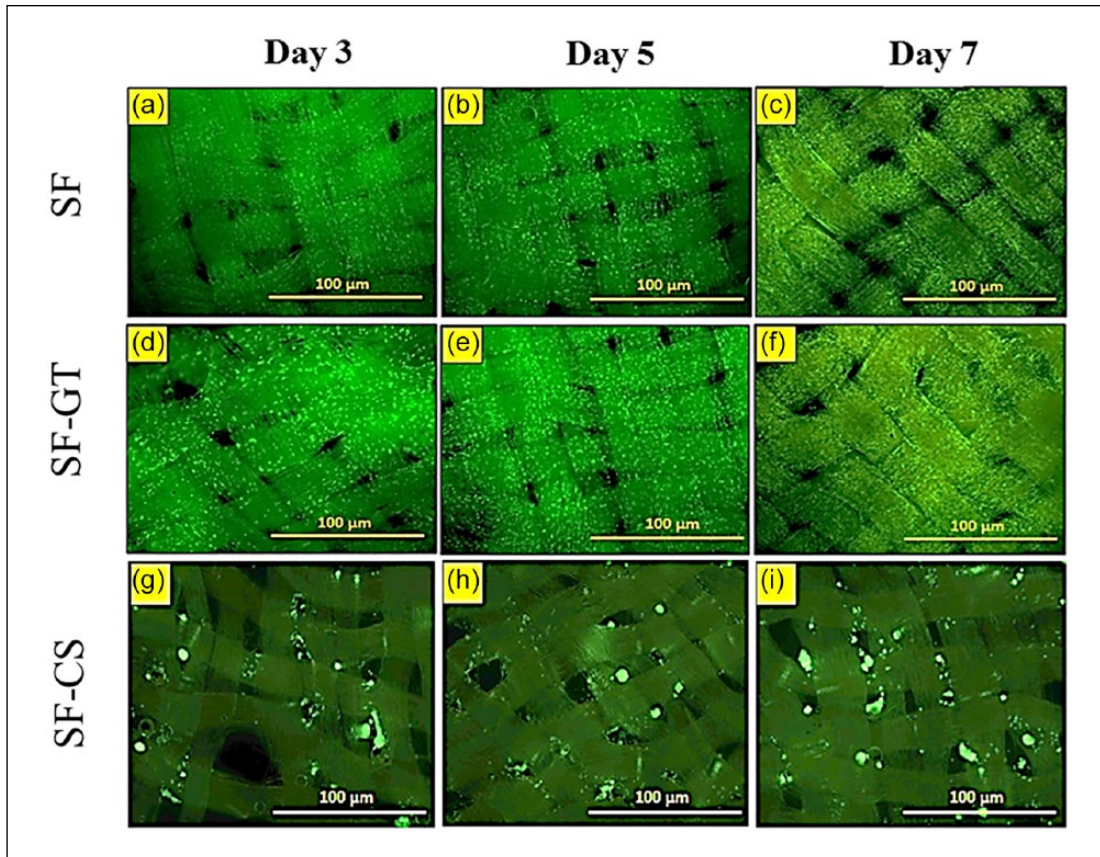


Figure 9. (a–c) Fibroblast cell viability staining with FDA on the silk fabric. (d–f) Gelatin-coated silk fabric. (g–i) Chitosan-coated silk fabric.

designed to be in contact with fibroblasts, while the second part was designed to be attached to keratinocytes. The main function of the first part is to act as a substrate to induce tissue formation from fibroblasts. The second part is intended to enhance tissue formation from keratinocytes.

In the case of the first part, the results from the morphological observations indicated that the gelatin and chitosan showed a thin layer that covered the bundles of fibers and a smooth film that covered the surface of the woven structure. The thin layer on the bundles of fibers and the smooth film on the woven fabric might be clues that indicate effects on the biological performance of mimicked anatomical scaffolds. Therefore, to clarify the crystal structure and the molecular organization is important to explain the structure–function relationship of those clues. In this research the XRD and DSC clarified the crystal structures and molecular organizations. The results revealed that gelatin and chitosan had amorphous structures related to the broad peak of XRD.³⁸ The results also demonstrated that the SF-CS showed a broader shoulder than the SF-GT. This indicated that the chitosan formed a more amorphous structure other than the gelatin. The DSC results further demonstrated that the SF had greater water structure and stability than the SF-GT and SF-CS. Interestingly, some research

demonstrated that the amorphous structures, water structure, and stability of the substrate are the clues that relate to the physical and biological performance of scaffolds.^{39,40}

Physical performance of the mimicked scaffolds

The swelling behavior, biodegradation, and mechanical properties were chosen to clarify the physical performance of mimicked scaffolds. With regard to the swelling behavior, the results demonstrated that the SF-GT had a greater unique swelling behavior than the others. This possibly arose from the unique, molecular flexibility in addition to the unstable gelatin which led to high water absorption, and which in turn had a greater effect on the swelling behavior than the SF-CS.⁴¹ Some studies have reported that the membranes inserted for mucosa reconstruction in the maxillofacial area needed to show suitable, physical function similar to natural tissue. The first physical performance requires that the membranes have a certain swelling behavior for tissue reconstruction similar to the native mucosa layer in the maxillofacial area.⁴² The second physical performance is degradation. The results demonstrated that the coating layer of gelatin had unique degradation. This was due first to its molecular characteristics that allow for easy enzyme

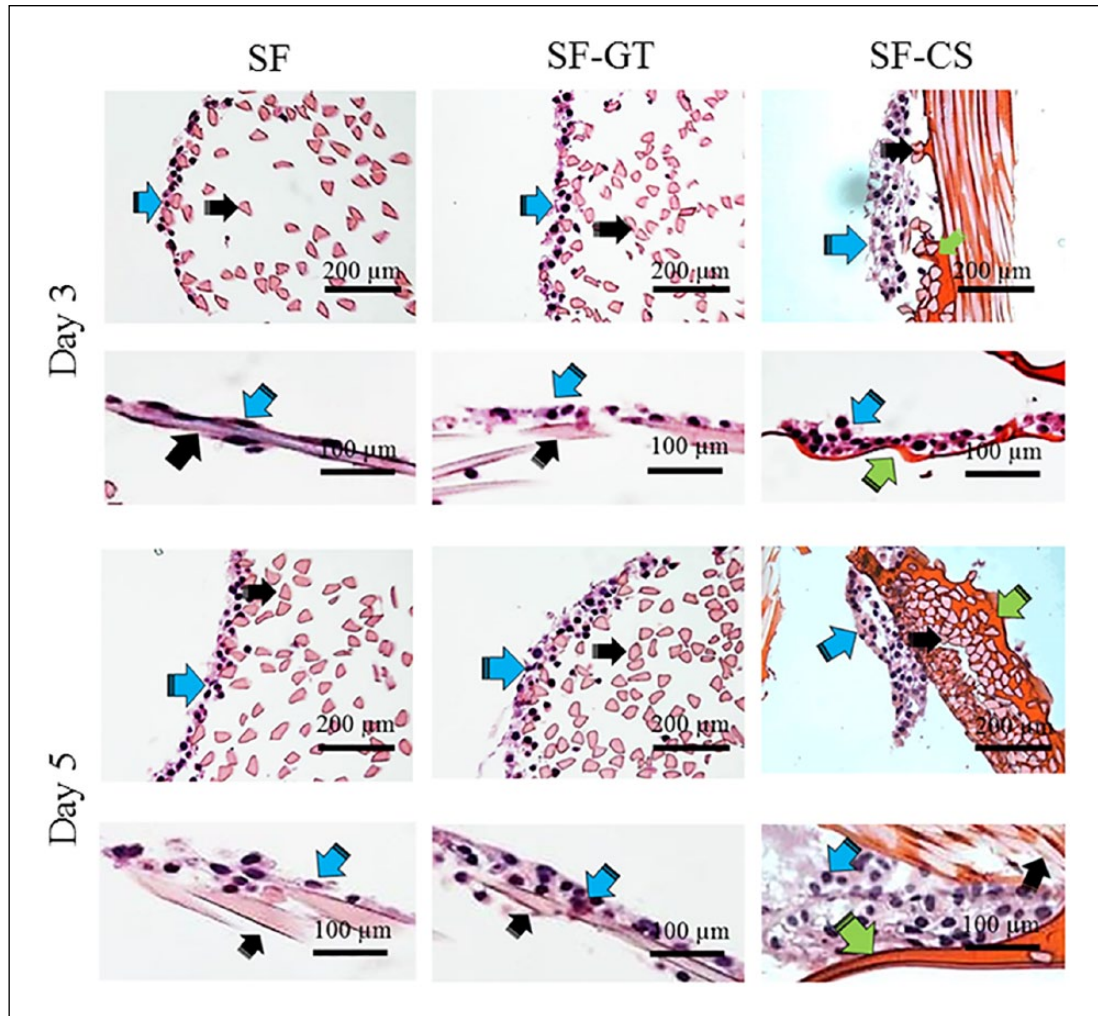


Figure 10. Fibroblast cell morphologies by H&E staining on days 3 and 5. Blue arrows indicate fibroblasts; black arrows indicate silk fibers, and green arrows indicate chitosan.

digestion.⁴³ The second reason comes from its molecular flexibility and the instability of gelatin. Interestingly, some research demonstrated that a certain degree of degradation of the scaffolds is important for the promotion of cell proliferation.⁴⁴ In this research, the coated woven silk fabrics could coincide with tissue formation of the native mucosa. The thin, coated layer represented the part in contact with the keratinocytes. Principally, that layer has to show a degradation period that is suitable for complete tissue regeneration.⁴⁵ However, silk fabric was proposed to be in contact with fibroblasts because silk fabric has a stable structure that can maintain the contour shape of the defect until the completion of the new tissue formation. Furthermore, silk fabric also has sufficient space for a fibroblast growth layer which is similar to the anatomical structure of natural, soft tissue. Notably, the thin coating layer that covered the fiber bundles of the silk fabric might be the clue to induce fibroblast cell adhesion with proliferation. However, to prove this a hypothesis was undertaken.

The mimicked scaffolds were tested for tensile behavior as the third physical performance. In the case of the SF-GT, the tensile behavior showed difficult extension at the early stage. This was possibly due to the effect of the gelatin coating on the surface. Gelatin has a unique functionality of adhesion, which can strictly bond to the silk fabric.⁴⁶ Then, for the second stage the coated silk fabrics of the SF-CS and GT showed a gradual increase in the stress, which then led to greater extension over the SF. This demonstrated that the chitosan adjoined with gelatin coatings disturbed the alignment of the fibers during extension. Therefore, the SF-GT plus CS had no rapid stress increase. In the last stage the results showed that the coated silk fabric broke at a greater extension point than the uncoated silk fabric. This indicated that chitosan, with a gelatin coating acted as a “shielding” force, and this shielding could prolong the breaking of the silk fabric to a greater extension point. The results of the mechanical behavior indicated that the coated fabrics had unique mechanical

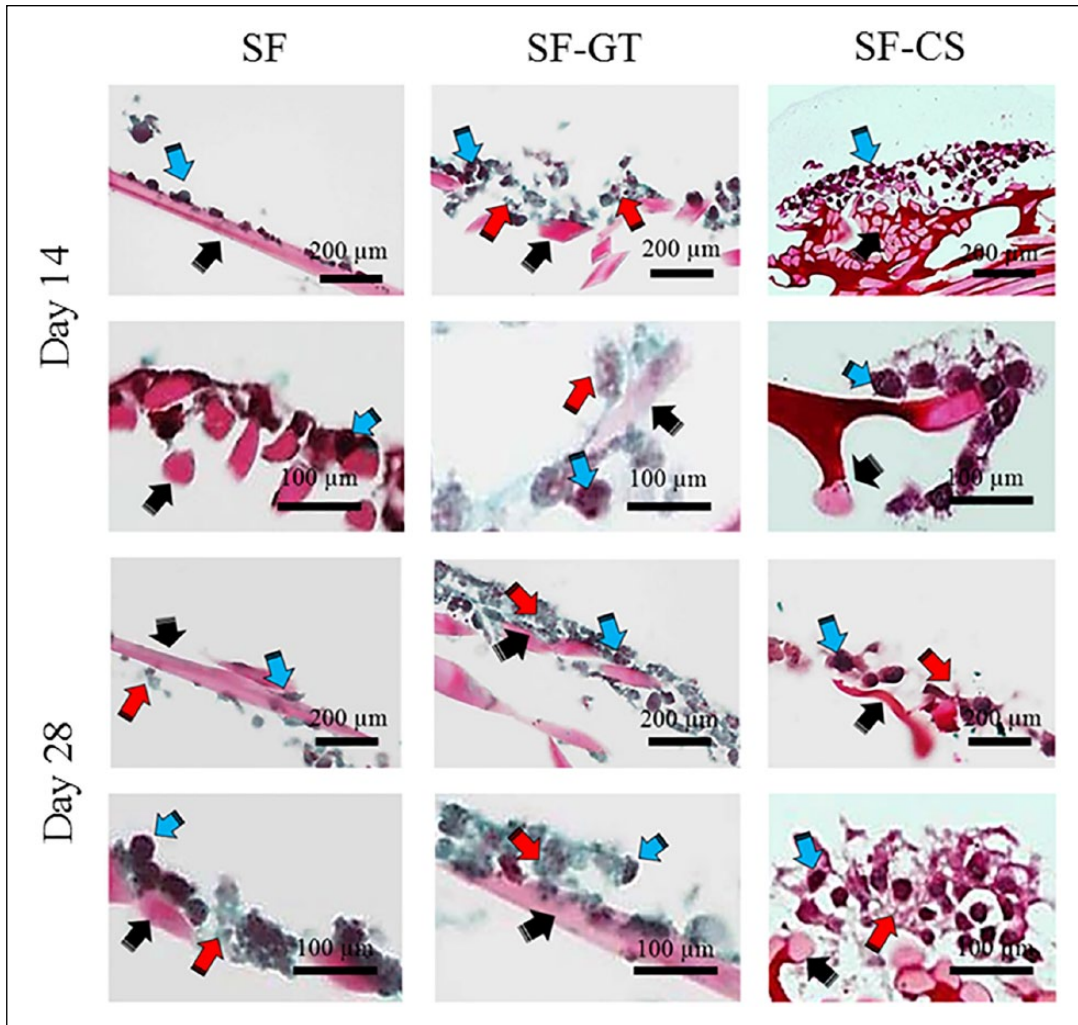


Figure 11. Masson's trichrome staining on days 14 and 28 to detect collagen deposition: black arrows indicate silk fibers, red arrows indicate the collagen matrix, and blue arrows indicate fibroblast cells.

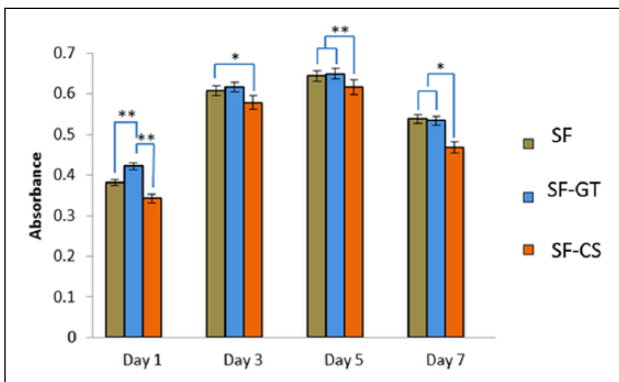


Figure 12. Keratinocyte cell proliferation in silk fabrics on days 1, 3, 5, and 7.

properties, especially SF-GT, which showed low Young's modulus and high strain at maximum load. This showed a flexible behavior similar to soft tissue.⁴⁷ The further results

indicated that the SF-GT had certain, mechanical characteristics for insertion into a defect area for soft tissue reconstruction.

Biological functionality of mimicked anatomical scaffolds

Cell viability, proliferation, and histology of the mimicked scaffolds were observed for biological functionality. The biological functionality of the mimicked scaffolds was evaluated by cell culturing. The uncoated layer of the scaffolds was tested with fibroblasts and the coated layer of silk fabric was tested with keratinocytes.

The results of cell viability and proliferation of the uncoated layers indicated that the fibroblasts rapidly adhered as well as proliferated in the early stages on the woven SF layer of the SF-GT. This was possibly due to the arginine-glycine-aspartate (RGD) groups, which can promote cell adhesion leading to enhanced cell viability and

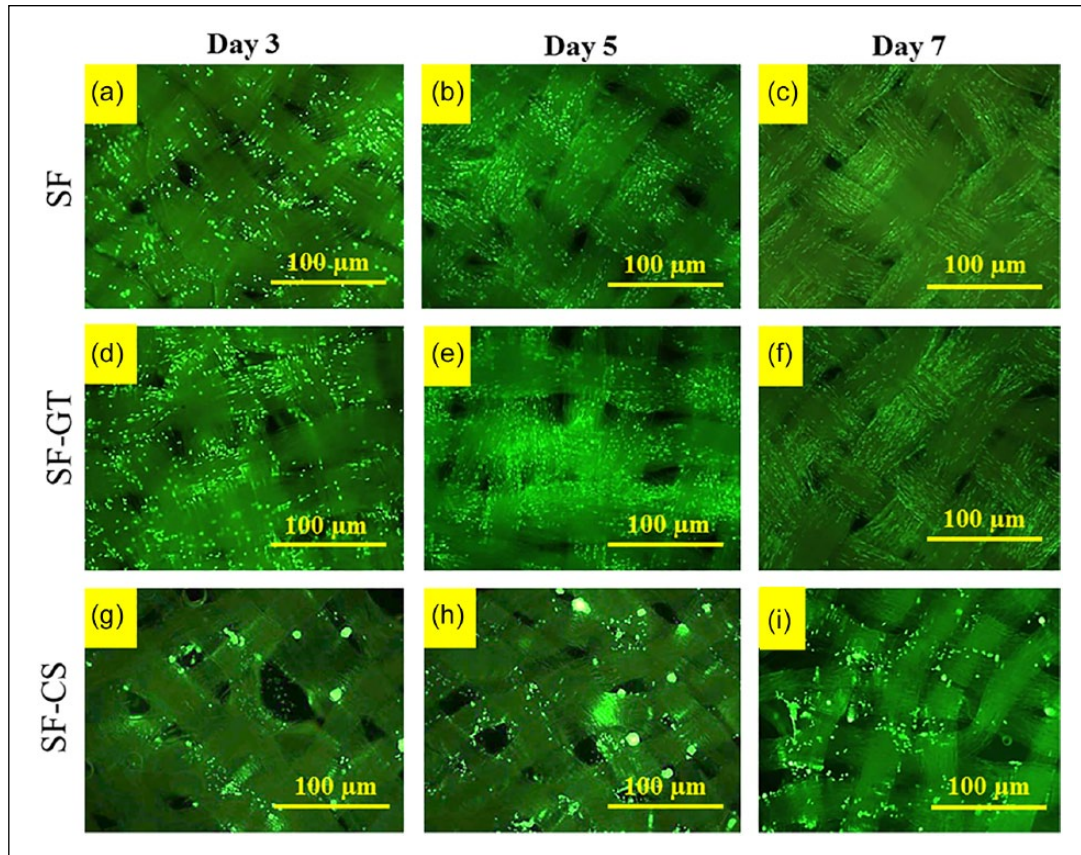


Figure 13. Keratinocyte cell viability staining with FDA. (a–c) Silk fabric. (d–f) Gelatin-coated silk fabric. (g–i) Chitosan-coated silk fabric at days 3, 5, and 7.

proliferation.⁴⁸ In the case of SF-CS, the results of cell viability and proliferation were not unique. This possibly arose because chitosan has no RGD groups. This led to less than desirable cell attachment, which resulted in decreased cell proliferation.

In the case of histological organization, the results indicated that the surfaces of the SF and SF-GT showed suitable structures and characteristics to promote both adhesion and elongation of the fibroblasts in the early stages of day 3. At the later stage of day 5, the unique migration of SF-GT possibly came from the free spaces of dissolved and degraded gelatin, during the culture period. Those free spaces could enhance cell migration.⁴⁹ In comparison, the dense clusters of cell aggregation of SF-CS were possibly due to the low degradation of chitosan, which covered the surface of the silk fabric. The low degradation led to the formation of fewer free spaces, which resulted in no cell migration into the fibrous bundles of the SF-CS. Importantly, the results demonstrated that the morphological formation of the SF-GT could induce cell adhesion. The fibrous, bundle structures promoted cell migration³⁹ which, in turn, led to cell adhesion and migration and enhancement in soft tissue regeneration.⁵⁰ The results demonstrated that the SF-GT induced collagen deposition

which was synthesized from the fibroblasts. A study reported that gelatin could stimulate collagen deposition from fibroblast cells by the RGD sequence and promote wound healing during soft tissue regeneration.⁷ However, the SF-CS had cell migration which covered some areas on the surface at all time points. This may have occurred because chitosan has no RGD groups which led to less cell adhesion and spherical formation of the cells.⁵¹

Interestingly, the SF-GT showed a suitable, biological function for soft tissue regeneration which would be suitable for surgery. For good surgical performance, the early stage for soft tissue regeneration of the fibroblasts, which are in the thick layer of the defect, should be provoked to express their functionality for maintaining contour shape. This supports the regular formation of the keratinocytes thin layer, which is sensitive to the lower layer organization of fibroblast.⁵²

The SF-GT had dominant cell viability and the highest amount of keratinocyte cell proliferation. A report demonstrated that RGD sequences in gelatin promoted cell proliferation along with the attachment of keratinocytes.⁵³ The results indicated that the layer of gelatin had suitable biological performance for soft tissue regeneration, particularly in the keratinocyte layer. Notably, in terms of surgical

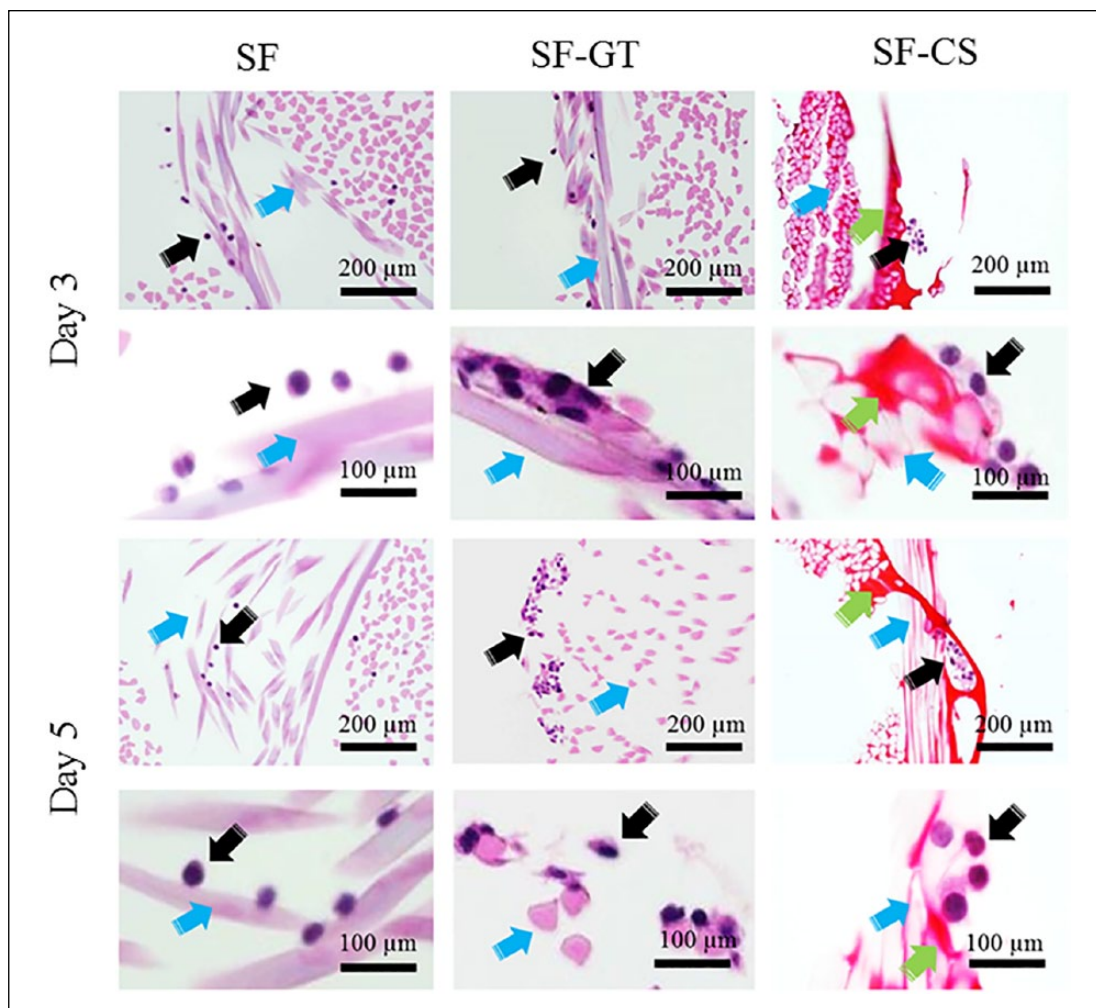


Figure 14. Keratinocyte cell morphologies on the silk fabric scaffolds on days 3 and 5, by H&E staining. The black arrows indicate keratinocyte cells, blue arrows indicate silk fibroin fibers, and green arrows indicate chitosan.

performance the gelatin layer can act as a temporary, boundary layer between the keratinocytes and fibroblasts. This temporary, boundary layer can possibly guide regular tissue formation at the interfacial area leading to a postoperative regular contour shape.⁵⁴

Conclusion

Mimicked anatomical scaffolds were fabricated with woven SF coated with gelatin and chitosan. The morphologies of the scaffolds were divided into two phases: woven SF and the coating layer. The woven SF layers showed covered fiber bundles with gelatin and chitosan. The coating layers, which covered the entire surfaces of the fabrics, had a twisted pattern of fiber bundles. The coated silk fabrics had a crystal structure of the silk fibroin, in addition to amorphous structures from the gelatin and chitosan. The coating layer of the gelatin showed a highly, stable water structure. The physical performance demonstrated that the coated woven SF with gelatin had suitable swelling behavior and biodegradation to perform as a scaffold for

reconstruction of soft tissue. The biological performance of the coated woven SF scaffold demonstrated suitable cell proliferation, viability, and morphology for reconstruction of soft tissue. Finally, this research demonstrated that mimicked anatomical scaffolds based on woven silk fibroin coated with gelatin have promising functionality for reconstruction of soft tissue in maxillofacial defect.

Acknowledgements

This work, conducted as a part of the Project REC.61-066-25-2, was supported by the Graduate School. The authors thank the Institute of Biomedical Engineering, Faculty of Medicine, and Queen Sirikit Sericulture Centre in Narathiwat for the supply of silk. The H357 keratinocytes used in this study were from an oral squamous carcinoma cell line and were gifted by Professor Paul Speight of the University of Sheffield, UK.

Declaration of conflicting interests

The author(s) declared no potential conflicts of interest with respect to the research, authorship, and/or publication of this article.

Funding

The author(s) received no financial support for the research, authorship, and/or publication of this article.

ORCID iD

Jirut Meesane  <https://orcid.org/0000-0002-6242-818X>

References

- Rai R, Raval R, Khandeparker RVS, et al. Tissue engineering: step ahead in maxillofacial reconstruction. *J Int Oral Health* 2015; 7(9): 138–142.
- Anura A. Traumatic oral mucosal lesions: a mini review and clinical update. *Oral Health Dent Manag* 2014; 13(2): 254–259.
- Gilvetti C, Porter SR and Fedele S. Traumatic chemical oral ulceration: a case report and review of the literature. *Br Dent J* 2010; 208(7): 297–300.
- d’Aquino R, DeRosa A, Lanza V, et al. Human mandible bone defect repair by the grafting of dental pulp stem/progenitor cells and collagen sponge biocomplexes. *Eur Cell Mater* 2009; 18: 75–83.
- Amini AR., Laurencin CT and Nukavarapu SP. Bone tissue engineering: recent advances and challenges. *Crit Rev Biomed Eng* 2012; 40(5): 363–408.
- Kanai N, Yamato M and Okano T. Cell sheets engineering for esophageal regenerative medicine. *Ann Transl Med* 2014; 2(3): 28–24.
- Schulz S, Angarano M, Fabritius M, et al. Nonwoven-based gelatin/polycaprolactone membrane proves suitability in a preclinical assessment for treatment of soft tissue defects. *Tissue Eng Part A* 2014; 20(13–14): 1935–1947. DOI: 10.1089/ten.TEA.2013.0594.
- Spicer P, Young S, Kasper FK, et al. Tissue engineering in oral and maxillofacial surgery. In: Lanza R, Langer R and Vacanti JP (eds) *Principles of tissue engineering*. 4th ed. New York: Academic Press, 2014, pp. 1487–1506.
- Stella JA, D’Amore A, Wagner WR, et al. On the biomechanical function of scaffolds for engineering load-bearing soft tissues. *Acta Biomater* 2010; 6(7): 2365–2381.
- Chen FM and Liu X. Advancing biomaterials of human origin for tissue engineering. *Prog Polym Sci* 2016; 53: 86–168.
- Kaur A, Midha S, Giri S, et al. Functional skin grafts: where biomaterials meet stem cells. *Stem Cells Int* 2019; 2019: 1286054.
- Li G, Li Y, Chen G, et al. Silk-based biomaterials in biomedical textiles and fiber-based implants. *Adv Healthc Mater* 2015; 4(8): 1134–1151.
- Kanokpanont S, Damrongsakkul S, Ratanavaraporn J, et al. An innovative bi-layered wound dressing made of silk and gelatin for accelerated wound healing. *Int J Pharm* 2012; 436(1–2): 141–153.
- Xie M, Xu Y, Song L, et al. Tissue-engineered buccal mucosa using silk fibroin matrices for urethral reconstruction in a caninemodel. *J Surg Res* 2014; 188(1): 1–7.
- Ha TLB, Quan TM, Vu DN, et al. Naturally derived biomaterials: preparation and application. In: Andradres JA (ed.) *Regenerative medicine and tissue engineering*. London: IntechOpen, 2013 pp. 247–274.
- Aduba DC, Hammer JA, Yuan Q, et al. Semi-interpenetrating network (sIPN) gelatin nanofiber scaffolds for mucosal drug delivery. *Acta Biomater* 2013; 9(5): 6576–6584.
- Murata Y, Isobe T, Kofuji K, et al. Development of oral dissolving gelatin beads containing allopurinol for the prevention and treatment of mucositis. *J Pharm Pharmacol* 2012; 3(3): 295–299.
- Croisier F and Jerome C. Chitosan-based biomaterials for tissue engineering. *Eur Polym J* 2013; 49(4): 780–792.
- Jayakumar R, Prabakaran M, SudheeshKumar PT, et al. Biomaterials based on chitin and chitosan in wound dressing applications. *Biotechnol Adv* 2011; 29(3): 322–337.
- Da Silva RM, Lopez-Perez PM, Elvira C, et al. Poly(N-isopropylacrylamide) surface-grafted chitosan membranes as a new substrate for cell sheet engineering and manipulation. *Biotechnol Bioeng* 2008; 101(6): 1321–1331.
- Imani R, Rafienia M, Emamia SH, et al. Synthesis and characterization of biodegradable hemostat gelatin sponge for surgery application. *Iran J Pharm Res* 2008; 4(3): 193–200.
- Hsu CH, Chen SK, Chen WY, et al. Effect of the characters of chitosans used and regeneration conditions on the yield and physicochemical characteristics of regenerated products. *Int J Mol Sci* 2015; 16(4): 8621–8634.
- Chang G, Kim HJ, Kaplan D, et al. Porous silk scaffolds can be used for tissue engineering annulus fibrosus. *Eur Spine J* 2007; 16(11): 1848–1857.
- Guziewicz N, Best AB, Perez-Ramirez B, et al. Lyophilized silk fibroin hydrogels for the sustained local delivery of therapeutic monoclonal antibodies. *Biomaterials* 2011; 32(10): 2642–2650.
- Mani S, Nair MB, Nisha S, et al. Adult stem cells on methacrylic acid grafted cocoon silky fibrous scaffolds. *Trends Biomater Artif Organs* 2010; 23(3): 137–144.
- Utto P, Piwat S and Teanpaisan R. Prevalence and adhesion properties of oral bifidobacterium species in caries-active and caries-free Thai children. *Walailak J Sci & Tech* 2017; 14(8): 645–653.
- Maarten S, Ioannis P, Frank PL, et al. Quantitative validation of the presto blue™ metabolic assay for online monitoring of cell proliferation in a 3d perfusion bioreactor system. *Tissue Eng Part C Methods* 2015; 21: 519–529.
- McDonald JA, Kelley DG and Broekelmann TJ. Role of fibronectin in collagen deposition: Fab’ to the gelatin-binding domain of fibronectin inhibits both fibronectin and collagen organization in fibroblast extracellular matrix. *J Cell Biol* 1982; 92(2): 485–492.
- Kasaju K, Kubies D, Kumorek MM, et al. Dip TIPS as a facile and versatile method for fabrication of polymer foams with controlled shape size and pore architecture for bioengineering applications. *PLoS ONE* 2014; 9(9): e108792.
- Farokhi M, Mottaghitalab F, Hadjati J, et al. Structural and functional changes of silk fibroin scaffold due to hydrolytic degradation. *J Appl Polym Sci* 2013; 131(6): 1–8.
- Nady N and Kandil SH. Novel blend for producing porous chitosan-based films suitable for biomedical applications. *Membranes (Basel)* 2018; 8(1): E2.
- Wang F, Wolf N, Rocks EM, et al. Comparative studies of regenerated water-based Mori, Thai, Eri, Muga and Tussah silk fibroin films. *J Therm Anal Calorim* 2015; 122(3): 1069–1076.

33. Motta A, Fambri L and Migliaresi C. Regenerated silk fibroin films: thermal and dynamic mechanical analysis. *Macromol Chemical Physics* 2002; 203(10–11): 1658–1665.
34. Sarasam A and Madihally SV. Characterization of chitosan-polylactone blends for tissue engineering applications. *Biomaterials* 2005; 26(27): 5500–5508.
35. Ratanavaraporn J, Damrongsakkul S, Sanchavanakit N, et al. Comparison of gelatin and collagen scaffolds for fibroblast cell culture. *J Metal Mater Miner* 2006; 16(1): 31–36.
36. Yamada H, Igarashi Y, Takasu Y, et al. Identification of fibroin-derived peptides enhancing the proliferation of cultured human skin fibroblasts. *Biomaterials* 2004; 25(3): 467–472.
37. Jaiswal AK, Dhupal RV, Ghosh S, et al. Bone healing evaluation of nanofibrous composite scaffolds in rat calvarial defects: a comparative study. *J Biomed Nanotechnol* 2013; 9(12): 2073–2085.
38. Jiang T, Zhang Z, Zhou Y, et al. Surface functionalization of titanium with chitosan/gelatin via electrophoretic deposition: characterization and cell behavior. *Biomacromolecules* 2010; 11(5): 1254–1260.
39. Qi Y, Wang H, Wei K, et al. A review of structure construction of silk fibroin biomaterials from single structures to multi-level structures. *Int J Mol Sci* 2017; 18(3): 237–258.
40. Mehta M, Kothari K, Ragoonanan V, et al. Effect of water on molecular mobility and physical stability of amorphous pharmaceuticals. *Mol Pharm* 2016; 13(4): 1339–1346.
41. Haider S, Park SY and Lee SH. Preparation, swelling and electro-mechano-chemical behaviors of a gelatin–chitosan blend membrane. *Soft Matter* 2008; 4: 485–492.
42. Gupta S, Pratibha PK and Richa G. Mucosal substitutes for periodontal soft tissue regeneration. *Dentistry* 2015; 5: 327.
43. Wang HM, Chou YT, Wen ZH, et al. Novel biodegradable porous scaffold applied to skin regeneration. *PLoS ONE* 2013; 8(6): e56330.
44. Liu J, Mao JJ and Chen L. Epithelial-mesenchymal interactions as a working concept for oral mucosa regeneration. *Tissue Eng Part B Rev* 2011; 17(1): 25–31.
45. O'Brien FJ. Biomaterials & scaffolds for tissue engineering. *Mater Today* 2011; 14(3): 88–95.
46. Marcolin C, Draghi L, Tanzi MC, et al. Electrospun silk fibroin-gelatin composite tubular matrices as scaffolds for small diameter blood vessel regeneration. *J Mater Sci Mater Med* 2017; 28(5): 80–12.
47. Lv J, Chen L, Zhu Y, et al. Promoting epithelium regeneration for esophageal tissue engineering through basement membrane reconstitution. *ACS Appl Mater Interfaces* 2014; 6(7): 4954–4964.
48. Bellis SL. Advantages of RGD peptides for directing cell association with biomaterials. *Biomaterials* 2011; 32(18): 4205–4210.
49. Lee JB, Ko YG, Cho D, et al. Modification and optimization of electrospun gelatin sheets by electron beam irradiation for soft tissue engineering. *Biomater Res* 2017; 21: 14–19.
50. Zhou T, Wang N, Xue Y, et al. Electrospun tilapia collagen nanofibers accelerating wound healing via inducing keratinocytes proliferation and differentiation. *Colloids Surf B Biointerfaces* 2016; 143: 415–422.
51. New N, Furuike T and Tamura H. The mechanical and biological properties of chitosan scaffolds for tissue regeneration templates are significantly enhanced by chitosan from *Gongronella butleri*. *Materials* 2009; 2(2): 374–398.
52. Wojtowicz AM, Oliveira S, Carlson MW, et al. The importance of both fibroblasts and keratinocytes in a bilayered living cellular construct used in wound healing. *Wound Repair Regen* 2014; 22(2): 246–255.
53. Zhao X, Lang Q, Yildirimer L, et al. Photocrosslinkable gelatin hydrogel for epidermal tissue engineering. *Adv Healthc Mater* 2016; 5(1): 108–118.
54. Chen S, Liu B, Carlson MA, et al. Recent advances in electrospun nanofibers for wound healing. *Nanomedicine (Lond)* 2017; 12(11): 1335–1352.